Reviews

Molecular structure of carbene analogs

M. Hargittai,[a]★ G. Schultz,[a] and I. Hargittai[a,b]

[a]*Structural Chemistry Research Group of the Hungarian Academy of Sciences at Eotvos University, Pf. 32, H-1518 Budapest, Hungary. Fax: 36 1 372 2731. E-mail: hargittaim@ludens.elte.hu*
[b]*Institute of General and Analytical Chemistry, Budapest University of Technology and Economics, H-1521 Budapest, Hungary. Fax: 36 1 463 4052. E-mail: hargittai@tki.aak.bme.hu*

The geometrical parameters of all carbene analogs, halocarbenes, and the corresponding tetrahalides obtained from experimental data and high-level quantum-chemical calculations were collected. Trends in their variations are interpreted using the VSEPR model and by consideration of the HOMOs and LUMOs.

Key words: carbenes, halocarbenes, carbene analogs, molecular structure, nonempirical quantum-chemical calculations.

The discovery of the tetrahedral bond configuration at the carbon atoms by van′t Hoff and Le Bel in 1874 was a breakthrough in the history of chemistry and it was also the starting point for the development of stereochemistry.[1] It was not an easy task to convince everybody of the validity of three-dimensional chemistry, but, over the decades, the tetracoordination of carbon has been strongly embedded in chemistry. The discovery, in the 1960s, of higher coordination carbon bond configurations (*e.g.*, in CH_5^+) by G. A. Olah[2] met hurdles, but by now its chemistry has also been established.

In the bond configurations, mentioned so far, as well as in the three-coordinated carbon characterized by sp^2 hybridization, all the electrons available in the valence shell of the carbon atom are involved in bonding. Carbene and its halogen derivatives provide a different pattern since in this case not all electrons in the valence shell of the two-coordinated carbon atom participate in bonding. Carbenes have two nonbonding electrons that can occupy two relatively low-lying orbitals, one with a_1 and the other with b_1 symmetry. In the two lowest-lying states, the electrons are arranged either in the $(a_1)^2$ configuration corresponding to the singlet state ($^1A_1$) or in the $(a_1)(b_1)$ configuration corresponding to the triplet state ($^3B_1$). Due to the divalence of the carbon atom, these species are highly reactive. The two different electronic states are also characterized by different chemical behavior and different geometries. Although the existence of carbene did not entice controversies, the relative stability of its states has been a question of debate for a long time. Carbenes, their halogen derivatives, and the related species formed by other Group 14 elements have been the focus of much research efforts for their unstable character, reactivity, and simply because they were a challenge to the structural chemists.

Published in Russian in *Izvestiya Akademii Nauk. Seriya Khimicheskaya,* No. 11, pp. 1817—1829, November, 2001.

1066-5285/01/5011-1903 $25.00

O. M. Nefedov and his associates have considerably contributed to the chemistry and structural chemistry of carbenes and carbene analogs (for references to our joint papers, see below). Their contributions have been characterized by a concerted application of various techniques of structure determination and by resourceful synthetic chemistry.

The present paper reviews the available experimental and computed data on the geometrical parameters of carbenes and carbene analogs, AX_2 (A = C, Si, Ge, Sn, Pb; X = H, F, Cl, Br, I), in their lowest-lying singlet and triplet states. From among the large number of computations, especially on carbene, only the best and relatively recent results are quoted. For comparison, we also report the bond lengths in the corresponding tetrahalides of Group 14 elements.

Most of the experimental studies were carried out by microwave spectroscopy, gas-phase electron diffraction, and laser-induced fluorescence spectroscopy. Different experimental techniques provide average structures with different physical meanings.[3] These average structures differ from the equilibrium structures obtained from quantum-chemical calculations, due to their different physical meaning. For proper comparison, vibrational corrections have to be applied to the average geometrical parameters. In the tables we give the proper physical meaning for all the parameters quoted. Parameters other than in the r_e representation can only be discussed in relation to the equilibrium parameters taking into account the appropriate vibrational corrections.

Table 1 presents the geometrical parameters and dipole moments of carbene and its halogen-analogs, CX_2 (X = H, F, Cl, Br, I) in their lowest-lying singlet ($^1A_1$) and triplet ($^3B_1$) states, obtained from experimental studies and from various *ab initio* and density functional (DFT) calculations. Analogous data for the non-carbon AX_2 (A = Si, Ge, Sn, Pb; X = H, F, Cl, Br, I) species are listed in Table 2. The experimental and calculated energy gaps between the ground and first excited states of these species are presented in Tables 3

Table 1. Experimental and calculated geometrical parameters and dipole moments (μ_e) of carbenes CX_2 (X = H, F, Cl, Br, and I) in their lowest-lying singlet ($^1A_1$) and triplet ($^3B_1$) states

Species (state)	r(C—X)/Å	Angle X—C—X /deg	μ_e/D	Physical meaning, method[a] /level of theory, basis sets	Reference
CH_2 ($^1A_1$)			Experiment		
	1.107(2)	102.4(4)		r_e, based on infrared flash-kinetic spectroscopy	4
			Calculations		
	1.109	102.0	1.809	B3LYP/6-311+G(3df,2p)	5
	1.109—1.133[b]	100.0—102.0[b]	1.76—1.96[b]	r_e [c]	5
	1.1168	101.5	1.1812	r_e, TCSCF-CISD/DZP	6
	1.1199	101.44	1.799	r_e, full CI/DZP	6
	1.1051	102.05	1.726	r_e, TCSCF-CISD/TZ2P	7
	1.1087	101.88	1.713	r_e, CISDTQ/TZ2P	7
	1.1089	101.89	1.711	r_e, full CI/TZ2P	7
	1.1047	102.3	1.690	r_e, TCSCF-CISD	8
	1.116	101.0		r_e, QCISD/6-311G(d,p)	9
	1.110	101.6		r_e, B3LYP/cc-pVTZ	10
	1.117	101.5		r_e, CCSD(T)/6-311++G(d,p)	11
	1.118	100.4		r_e, LCGTO-LSD	12
CH_2 ($^3B_1$)			Experiment		
	1.078	~136		r_0, UV	13
	1.0766(14)	134.037(45)		r_e, MW + IR	14
			Calculations		
	1.077	135.2	0.612	r_e, B3LYP/6-311+G(3df,2p)	5
	1.077—1.097[b]	133.4—137.2[b]	0.600—0.751[b]	r_e [c]	5
	1.085	131.79	0.646	r_e, CISD/DZP	6
	1.087	132.16	0.651	r_e, CISDTQ/DZP	6
	1.077	133.29	0.602	r_e, CISDTQ/TZ2P	7
	1.077	133.29	0.602	r_e, full CI/TZ2P	7
	1.087	132.16		r_e, full CI/DZP	6
	1.074	133.72		r_e, CMRCI	15
	1.075	133.82		r_e, RCCSD(T)	15
	1.083	132.6		r_e, QCISD/6-311G(d,p)	9
	1.077	135.0		r_e, B3LYP/cc-pVTZ	10
	1.084	133.1		r_e, CCSD(T)/6-311++G(d,p)	11
	1.084	135.4		r_e, LCGTO-LSD	12

(*to be continued*)

Table 1 (*continued*)

Species (state)	r(C—X)/Å	Angle X—C—X /deg	μ_e/D	Physical meaning, method[a] /level of theory, basis sets	Reference
CF_2 ($^1A_1$)			Experiment		
	1.3035(1)	104.778(20)	0.469(26)	r_0, MW	16
	1.300	104.94		r_0, UV	17
			Calculations		
	1.300	104.8	0.588	r_e, B3LYP/6-311+G(3df)	5
	1.296—1.329[b]	104.2—104.7[b]	0.577—0.644[b]	r_e[c]	5
	1.276	105.0		r_e, DDCI	18
	1.302	104.7		r_e, QCISD/6-311G(d,p)	9
	1.3048	104.1		r_e, B3LYP/QR	19
	1.299	104.7		r_e, CASSCF	20
	1.300	105.2		r_e, CASPT2	20
	1.303	104.9		r_e, CCSD(T)	20
	1.303	104.79		r_e, B3LYP/6-311+G(2df)	21
	1.30	104.91		r_e, MP2/6-311+G*	22
	1.307	104.7		r_e, CCSD(T)/6-311++G(d,p)	11
	1.315	103.9		r_e, LCCGTO-LSD	12
CF_2 ($^3B_1$)			Calculations		
	1.314	119.6	0.347	r_e, B3LYP/6-311+G(3df)	5
	1.307—1.339[b]	119.5—120.0[b]	0.22—0.397[b]	r_e [c]	5
	1.298	118.1		r_e, DDCI	18
	1.318	119.5		r_e, QCISD/6-311G(d,p)	9
	1.318	119.2		r_e, CASSCF	20
	1.315	119.6		r_e, CASPT2	20
	1.317	119.4		r_e, CCSD(T)	20
	1.321	119.1		r_e, CCSD(T)/6-311++G(d,p)	11
	1.32	119.16		r_e, MP2/6-311+G*	22
	1.322	119.0		r_e, LCGTO-LSD	12
CCl_2 ($^1A_1$)			Experiment		
	1.7157(28)	109.2(3)		r_0, MW	23
	1.714(1)	109.3(1)		r_0, LIF	24
			Calculations		
	1.720	109.1		r_e, CCSD(T)/cc-pVQZ	25
	1.722	109.9	1.106	r_e, B3LYP/6-311+G(3df)	5
	1.709—1.780[b]	109.3—109.8[b]	1.00—1.196[b]	r_e [c]	5
	1.704	110.1		r_e, DDCI	18
	1.730	110.0		r_e, QCISD/6-311G(d,p)	9
	1.7525	109.1		r_e, B3LYP/QR	19
	1.751	109.5		r_e, CASSCF	20
	1.727	109.2		r_e, CAPST2	20
	1.731	109.1		r_e, CCSD(T)	20
	1.730	110.0		r_e, CCSD(T)/6-311++G(d,p)	11
	1.71	110.36		r_e, MP2/6-311+G*	22
	1.736	109.3		r_e, LCCGTO-LSD	12
CCl_2 ($^3B_1$)			Calculations		
	1.675	127.7		r_e, CCSD(T)/cc-pVQZ	25
	1.672	128.9	0.336	r_e, B3LYP/6-311+G(3df)	5
	1.661—1.693[b]	127.8—129.0[b]	0.307—0.486[b]	r_e [c]	5
	1.687	126.1		r_e, DDCI	18
	1.689	127.5		r_e, QCISD/6-311G(d,p)	9
	1.710	127.2		r_e, CASSCF	20
	1.676	128.3		r_e, CASPT2	20
	1.685	127.8		r_e, CCSD(T)	20
	1.690	127.5		r_e, CCSD(T)/6-311++G(d,p)	11
	1.68	127.5		r_e, MP2/6-311+G*	22
	1.683	127.6		r_e, LCGTO-LSD	12

(*to be continued*)

Table 1 (*continued*)

Species (state)	r(C—X)/Å	Angle X—C—X /deg	μ_e/D	Physical meaning, method[a] /level of theory, basis sets	Reference
CBr_2 ($^1A_1$)			Experiment		
	1.74[d]	~112.0		r_a, ED	26
			Calculations		
	1.898	110.7	1.074	r_e, B3LYP/6-311+G(3df)	5
	1.881—1.953[b]	110.2—110.7[b]	0.984—1.129[b]	r_e [c]	5
	1.911	110.7		r_e, QCISD/6-311G(d,p)	9
	1.883	110.6		r_e, DDCI	18
	1.9167	110.2		r_e, B3LYP/QR	19
	1.926	110.3		r_e, CASSCF	20
	1.882	110.0		r_e, CASTP2	20
	1.898	110.0		r_e, CCSD(T)	20
	1.903	110.5		r_e, CCSD(T)/6-311++G(d,p)	11
	1.88	110.66		r_e, MP2/6-311+G*	22
	1.893	112.4		r_e, LCGTO-LSD	12
CBr_2 ($^3B_1$)			Experiment		
	1.74[d]	~150		r_a, ED	26
			Calculations		
	1.839	130.1	0.487	r_e, B3LYP/6-311+G(3df)	5
	1.824—1.873[b]	129.5—130.1[b]	0.458—0.715[b]	r_e [c]	5
	1.859	127.7		r_e, DDCI	18
	1.852	129.8		r_e, QCISD/6-311G(d,p)	9
	1.868	129.0		r_e, CASSCF	20
	1.816	130.2		r_e, CASPT2	20
	1.839	129.5		r_e, CCSD(T)	20
	1.847	129.7		r_e, CCSD(T)/6-311++G(d,p)	11
	1.84	129.27		r_e, MP2/6-311+G*	22
	1.837	128.9		r_e, LCGTO-LSD	12
CI_2 ($^1A_1$)			Experiment		
	2.085(13)	112.3[e]		r_g, ED	27
			Calculations		
	2.123	112.6		r_e, QCISD/6-311G(d,p)	9
	2.1496	111.9		r_e, B3LYP/QR	19
	2.114	112.0		r_e, LCGTO-LSD	12
	2.101	111.2		r_e, LDA	28
	2.074	112.3		r_e, MP2	27
	2.103	112.4		r_e, MP2(FC)	27
	2.105	112.6		r_e, MP2	29
	2.120	112.4		r_e, CCSD(T)	30
	2.135	112.3		r_e, CCSD(T)/6-311++G(d,p)	11
	2.09	112.66		r_e, MP2/LanL2DZ	22
CI_2 ($^3B_1$)			Experiment		
	2.029(7)	132[e]		r_g, ED	27
			Calculations		
	2.038	132.9		r_e, QCISD/6-311G(d,p)	9
	2.025	132.7		r_e, LCGTO-LSD	12
	2.034	131.5		r_e, LDA	28
	2.018	132.0		r_e, MP2	27
	2.045	131.7		r_e, MP2(FC)	27
	2.034	132.3		r_e, MP2	29
	2.042	133.2		r_e, CCSD(T)	30
	2.059	132.0		r_e, CCSD(T)/6-311++G(d,p)	11
	2.03	132.2		r_e, MP2/LanL2DZ	22

[a] Notations: UV, MW, and IR stand for ultraviolet, microwave, and infrared spectroscopy, respectively; LIF stands for laser-induced fluorescence; and ED stands for electron diffraction.
[b] Depending on the level of theory and basis set.
[c] See reference for details.
[d] Probably in error.
[e] Fixed value.

Table 2. Experimental and calculated geometrical parameters and dipole moments (μ_e) of carbene analogs AX_2 (A = Si, Ge, Sn, and Pb; X = H, F, Cl, Br, and I) in their lowest-lying singlet ($^1A_1$) and triplet ($^3B_1$) states

Species (state)	r(A—X)/Å	Angle X—A—X /deg	μ_e/D	Physical meaning, method /level of theory, basis sets	Reference
SiH_2 ($^1A_1$)			Experiment		
	1.5140	92.08		r_e, IR	31
	1.51402	91.9830		r_e, ICLAS	32
			Calculations		
	1.517	92.3		r_e, CCSD(T)/aV5Z	33
	1.519	92.5		r_e, SOCI-f(D)	34
	1.524	92.3		r_e, MP2/DZP	35
SiH_2 ($^3B_1$)			Calculations		
	1.480	118.4		r_e, CCSD(T)/aV5Z	33
	1.484	118.5		r_e, SOCI-f(D)	34
SiF_2 ($^1A_1$)			Experiment		
	15901(1)	100.76(2)	1.230(15)	r_e, MW	36
			Calculations		
	1.599	100.5		r_e, CCSD(T)/aV5Z	33
	1.6149	100.2		r_e, B3LYP/QR	19
	1.584	99.9		r_e, CISD	37
	1.590	99.0		r_e, CASPT2	38
	1.640	100.2		r_e, MP2/DZP	35
SiF_2 ($^3B_1$)			Experiment		
	1.586(1)	113.1(1)		r_0, LIP	39
			Calculations		
	1.581	113.3		r_e, CISD	37
	1.586	113.1		r_e, MRSDCI	40
	1.586	110.9		r_e, CASPT2	38
$SiCl_2$ ($^1A_1$)			Experiment		
	2.088(4)	102.8(6)		r_g, ED	41
	2.076(4)	104.2(6)		r_e, ED + SP	42
	2.065310(26)	101.3240(16)		r_e, MW	43
			Calculations		
	2.102	101.4		r_e, HF	44
	2.1138	102.0		r_e, B3LYP/QR	19
	2.073	101.7		r_e, MP2/6-31G**	45
	2.094	101.5		r_e, MP2/DZP	35
$SiCl_2$ ($^3B_1$)			Experiment		
	2.041(5)	114.5 or 115.4		r_e, based on emission spectra	46
			Calculations		
	2.073	116.92		r_e, HF	44
	2.049	118.2		r_e, UMPP2/6-31G**	45
$SiBr_2$ ($^1A_1$)			Experiment		
	2.249(5)	102.7(3)		r_g, ED	41
	2.227(6)	103.1(4)		r_e, ED + SP	42
			Calculations		
	2.257	102.16		r_e, HF	44
	2.2847	103.0		r_e, B3LYP/QR	19
	2.257	102.2		r_e, MP2/DZP	35
$SiBr_2$ ($^3B_1$)			Calculations		
	2.219	118.5		r_e, HF	44
SiI_2 ($^1A_1$)			Calculations		
	2.5324	104.6		r_e, B3LYP/QR	19
GeH_2 ($^1A_1$)			Experiment		
	1.591(7)	91.2(8)		r_0, LIP	47
			Calculations		
	1.603	90.69	0.2904	r_e, B3LYP/6-311G*	48
	1.587	91.5	0.1586	r_e, MCSCF/SOCI/RCI	49
GeH_2 ($^3B_1$)			Calculations		
	1.545	119.8		r_e, CASSCF	47
	1.534	119.8		r_e, MCSCF/SOCI/RCI	49

(*to be continued*)

Table 2 (*continued*)

Species (state)	r(A—X)/Å	Angle X—A—X /deg	μ_e/D	Physical meaning, method /level of theory, basis sets	Reference
GeF_2 ($^1A_1$)			Experiment		
	1.7321(2)	97.148(30)		r_e, MW	50
			Calculations		
	1.745	97.2		r_e, BHLYP	51
	1.772	98.4		r_e, B3LYP	51
	1.770	98.37	2.681	r_e, B3LYP/6-311G*	48
	1.7771	97.8		r_e, B3LYP/QR	19
	1.723	97.1	2.450	r_e, MRSDCI+(Q)	52
	1.732	97.6		r_e, CCSD/DZP(2f)	53
	1.761	97.5		r_e, DFT	54
GeF_2 ($^3B_1$)			Calculations		
	1.715	113.1	2.240	r_e, MRSDCI+(Q)	52
	1.727	113.6		r_e, CCSD/DZP(2f)	53
	1.748	112.0		r_e, DFT	54
$GeCl_2$ ($^1A_1$)			Experiment		
	2.186(4)	100.3(4)		r_g, ED	55
	2.16945(2)	99.8825(15)		r_e, MW	56
			Calculations		
	2.177	100.35		r_e, HF	44
	2.218	101.1	2.615	r_e, B3LYP/6-311G*	48
	2.2359	100.9		r_e, B3LYP/QR	19
	2.191	100.5	2.956	r_e, MRSDCI	57
	2.212	97.5		r_e, DFT	54
$GeCl_2$ ($^3B_1$)			Calculations		
	2.145	117.30		r_e, HF	44
	2.040	118.6	1.653	r_e, MRSDCI	57
	2.180	116.0		r_e, DFT	54
$GeBr_2$ ($^1A_1$)			Experiment		
	2.359(5)	101.0(3)		r_g, ED	58
			Calculations		
	2.327	101.49		r_e, HF	44
	2.379	102.2	2.209	r_e, B3LYP 6-311G*	48
	2.3919	102.3		r_e, B3LYP/QR	19
	2.373	101.8	2.394	r_e, MRSDCI	57
	2.355	98.0		r_e, DFT	54
$GeBr_2$ ($^3B_1$)			Calculations		
	2.287	118.73		r_e, HF	44
	2.348	120.8	1.143	r_e, MRSDCI	57
	2.349	115.0		r_e, DFT	54
GeI_2 ($^1A_1$)			Experiment		
	2.540(5)	102.1(10)		r_α, ED	59
			Calculations		
	2.6242	104.4		r_e, B3LYP/QR	19
	2.574	102.8	1.422	r_e, MRSDCI	57
GeI_2 ($^3B_1$)			Calculations		
	2.556	122.3	0.569	r_e, MRSDCI	57
SnH_2 ($^1A_1$			Calculations		
	1.785	91.1	0.554	r_e, MCSCF/SOCI/RCI	49
SnH_2 ($^3B_1$)			Calculations		
	1.730	114.9		r_e, MCSCF/SOCI/RCI	49
SnF_2 ($^1A_1$)			Calculations		
	1.9477	96.0		r_e, B3LYP/QR	19
	1.865	92.0	3.306	r_e, MRSDCI+Q	52
SnF_2 ($^3B_1$)			Calculations		
	1.858	112.9	3.137	r_e, MRSDCI+Q	52

(*to be continued*)

Table 2 (*continued*)

Species (state)	r(A—X)/Å	Angle X—A—X /deg	μ_e/D	Physical meaning, method /level of theory, basis sets	Reference
$SnCl_2$ ($^1A_1$)			Experiment		
	2.345(3)	98.5(20)		r_g, ED	60
	2.338(3)	97.7(8)		r_e, ED + SP	61
	2.335(3)	99.1(20)		r_e, ED + SP	62
			Calculations		
	2.4166	98.9		r_e, B3LYP/QR	19
	2.394	98.9		r_e, CASSCF	63
	2.363	98.4	3.739	r_e, MRSDCI	63
	2.367	98.5		r_e, MP2	64
	2.374	98.5		r_e, QCISD	64
$SnCl_2$ ($^3B_1$)			Calculations		
	2.362	115.0		r_e, CASCF	63
	2.336	116.0	2.684	r_e, MRDSCI	63
$SnBr_2$ ($^1A_1$)			Experiment		
	2.512(3)	99.7(20)		r_g, ED	65
	2.501(3)	100.0(20)		r_e, ED + SP	62
	2.504(3)	98.6(7)		r_e, ED + SP	61
			Calculations		
	2.567	100.0		r_e, B3LYP/QR	19
	2.552	100.3		r_e, CASCF	63
	2.535	99.7	3.400	r_e, MRSDCI	63
	2.529	99.5		r_e, MP2	64
	2.536	99.4		r_e, QCISD	64
$SnBr_2$ ($^3B_1$)			Calculations		
	2.525	118.7		r_e, CASCF	63
	2.511	119.8	1.976	r_e, MRSDCI	63
SnI_2 ($^1A_1$)			Experiment		
	2.706(4)			r_g, ED	65
	2.688(6)	105.3		r_e, ED + SP	62
	2.699(3)	103.5(9)		r_e, ED + SP	61
			Calculations		
	2.7955	102.3		r_e, B3LYP/QR	19
	2.772	101.6		r_e, CASCF	63
	2.738	100.9	2.863	r_e, MRDSCI	63
	2.752	100.7		r_e, MP2	64
SnI_2 ($^3B_1$)			Calculations		
	2.747	120.8		r_e, CASCF	63
	2.718	121.4	1.335	r_e, MRDSCI	63
PbH_2 ($^1A_1$)			Calculations		
	1.828	92.1		r_e, HF/QRPP	66
	1.896	90.5	1.368	r_e, MCSCF/SOCI/RCI	49
PbH_2 ($^3B_1$)			Calculations		
	1.844	119.5		r_e, MCSCF/SOCI/RCI	49
PbF_2 ($^1A_1$)			Experiment		
	2.036(3)	96.2(22)		r_g, ED	60
	2.041(3)			r_g, ED	67
			Calculations		
	2.027	95.8		r_e, HF/QRPP	66
	2.0183	95.8		r_e, B3LYP/QR	19
	2.139	98.5	5.669	r_e, MRSDCI+Q	52
PbF_2 ($^3B_1$)			Calculations		
	2.131	126.2	2.588	r_e, MRSDCI+Q	52
$PbCl_2$ ($^1A_1$)			Experiment		
	2.447(5)	98.7(10)		r_g, ED	68
	2.444(5)	98.0(14)		r_g, ED	68
			Calculations		
	2.494	99.3		r_e, HF/QRPP	66
	2.505	99.8		r_e, B3LYP/QR	19
	2.552	100.3		r_e, CASCF	63
	2.542	100.8	5.289	r_e, MRSDCI	63

(*to be continued*)

Table 2 (*continued*)

Species (state)	r(A—X)/Å	Angle X—A—X /deg	μ_e/D	Physical meaning, method /level of theory, basis sets	Reference
$PbCl_2$ ($^3B_1$)			Calculations		
	2.586	127.1		r_e, CASSCF	63
	2.599	139.9	1.839	r_e, MRDSCI	63
$PbBr_2$ ($^1A_1$)			Experiment		
	2.597(3)	99.9(10)		r_g, ED	69
			Calculations		
	2.6485	100.8		r_e, B3LYP/QR	19
	2.685	101.4		r_e, CASCF	63
	2.684	101.5	5.038	r_e, MRDSCI	63
$PbBr_2$ ($^3B_1$)			Calculations		
	2.720	125.0		r_e, CASCF	63
	2.720	132.4	1.972	r_e, MRDSCI	63
PbI_2 ($^1A_1$)			Experiment		
	2.804(4)	99.9(12)		r_g, ED	60
			Calculations		
	2.8656	103.0		r_e, B3LYP/QR	19
	2.887	102.6		r_e, CASCF	63
	2.878	103.6	4.277	r_e, MRDSCI	63
PbI_2 ($^3B_1$)			Calculations		
	2.933	128.4		r_e, CASCF	63
	2.938	132.6	1.435	r_e, MRDSCI	63

Note. For abbreviations of experimental methods, see note to Table 1; LIP is laser-induced phosphorescence; and ED + SP is joint electron diffraction and vibrational spectroscopic analysis.

and 4, respectively. Finally, Table 5 gives the bond lengths in the molecules of all tetrahalides, AX_4, of Group 14 elements.

The computed bond lengths for carbene and its halogen derivatives are in good agreement with the experimental values, when available. The only exception is CBr_2 for which the experimental electron diffraction data[26] are probably in error (Fig. 1). For the heavier species the computed bond lengths are usually several hundredths of an Ångstrøm larger than the estimated experimental equilibrium bond lengths; they are often even larger than the thermal-average distances. Apparently, higher-level computations and better basis sets are needed to get more reliable theoretical estimates. The computed bond lengths for the triplet carbenes and their analogs are presented in Fig. 2. The bond length variations are consistent with the expectations, both for the same central atom with changing substituents from H to I, and for the same substituent with changing the central atom down the group in the periodic table, that is, the bond lengths increase in both cases.

The experimental data on the bond angle variation in the singlet AX_2 species exhibit a rather wide scatter (Fig. 3), especially for some of the heavier dihalides. This is due to the fact that the contribution of the nonbonded distances to the diffraction pattern has an

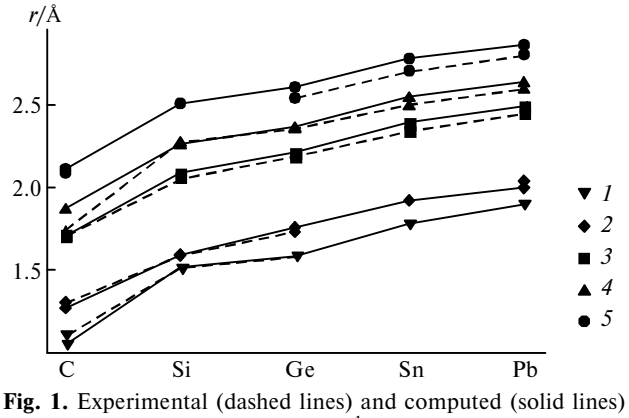

Fig. 1. Experimental (dashed lines) and computed (solid lines) bond length variations in singlet ($^1A_1$) carbenes and carbene analogs AX_2 (A = C, Si, Ge, Sn, Pb): X = H (*1*), F (*2*), Cl (*3*), Br (*4*), and I (*5*).

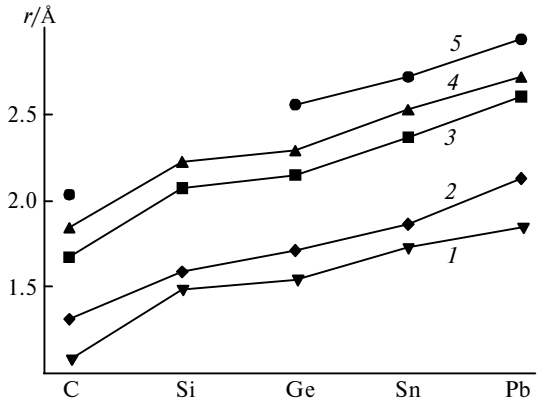

Fig. 2. Bond length variations in triplet ($^3B_1$) carbenes and carbene analogs AX_2 (A = C, Si, Ge, Sn, Pb): X = H (*1*), F (*2*), Cl (*3*), Br (*4*), and I (*5*) from computations.

Table 3. Experimental and calculated singlet—triplet energy gaps (ΔE_{S-T}) for carbenes CX_2 (X = H, F, Cl, Br, and I)

Species	ΔE_{S-T}[a] kJ mol^{-1}	$\Delta E_{S-T}{}^{0}$[b] kJ mol^{-1}	Method of determination[c]	Reference
CH_2			Experiment	
	−38.55(6)	−37.64(6)	Rotation-vibration spectroscopy data	70
			Calculations	
	−41.547	−39.982	ROB3LYP/aug-cc-pVDZ	5
	−47.17	−45.68	B3LYP/6-311+G(3df,2p)	5
	−52.98	−50.90	Full CI/DZP	6
	−46.14	−44.14	TC-CISD/TZ2P	7
	−46.99	−44.94	CISDTQ/TZ2P	7
	−39.480	−37.760	TC-CISD	8
	−41.62		RCCSD(T)	15
	−38.45		CMRCI	15
	−40.6		QCCISD(T)	9
	−43.17		CCSD(T)/cc-pVTZ	10
		−40.4	CCSD(T)/6-311++G(3df,2p)	11
		−38.6	CCSD(T)/aug-cc-pVTZ	11
	−38.07	−36.40	LCGTO-LSD/NLC	12
	−38.49		CCSD(T)/cc-pVQZ	20
	−30.12		LDA/NL	28
CF_2			Experiment	
	225.9(125)		NIPS	22
			Calculations	
	219.8	219.5	B3LYP/6-311+G(3df)	5
	235.9	235.5	DDCI	18
	234.4		QCISD(T)	9
	226.3	225.9	LCGTO-LSD/NLC	12
	232.6		LDA/NL	28
	236.14		CCSD(T)	10
	233.5		MRCI+Dav/cc-pVTZ	20
		235.1	CCSD(T)/6-311++G(3df,2p)	11
		236.3	CCSD(T)/aug-cc-pVTZ	11
CCl_2			Experiment	
	12.5(125)		NIPS	22
			Calculations	
	71.96	82.42	DDCI	18
	71.6	72.5	B3LYP/6-311+G(3df)	5
	82.2		QCISD(T)	9
	82.67		CCSD(T)	10
	97.9	99.16	LCGTO-LSD/NLC	12
		87.67	CCSD(T)/cc-pVQZ	20
		80.536	MRCI+Dac/cc-pVTZ	20
		82.8	CCSD(T)/6-311++G(3df,2p)	11
		59.2	CASPT2	11
	99.37		LDA/NL	28
	80.75		CCSD(T)/cc-pVTZ	25
CBr_2			Experiment	
	8.37(125)		NIPS	22
			Calculations	
	58.5	59.5	B3LYP/6-311+G(3df)	5
	60.24	65.27	DDCI	18
	63.1		CISD(T)	9
	77.40	77.40	LGTO-LSD/NLC	12
		54.57	CASPT2[g_1]/cc-pVTZ	20
		53.0	MP2/6-311++G(d,p)	11
	93.76		LDA/NL	28
CI_2			Experiment	
	−4.2(125)		NIPS	22
			Calculations	
	81.6(84)		CCSD(T)/cc-pCVQZ	25
	36.8		QCISD(T)	9
		46.8	MP4	29
	64.0		LGTO-LSD/NLC	12
	34.73		MP2	27
		49.2	CCSD(T)/6-311++G(3df,2p)	11
	68.99		LDA/NL	28

[a] Without inclusion of zero-point vibrational energy correction; the experimental error of determination is given in parentheses.
[b] With inclusion of zero-point vibrational energy correction.
[c] NIPS is negative-ion photoelectron spectroscopy.

increasingly diffuse character as a consequence of their large vibrational amplitudes. This effect is enhanced with increasing experimental temperature, which makes the results of electron diffraction studies uncertain. On the other hand, the computed data, except for PbH_2, show a definite trend (see Fig. 3). The bond angles decrease as we go from carbon to tin with the same substituent X, but they increase for lead. A decrease in the bond angles with decreasing electronegativity of the central atoms can be explained using, *e. g.*, the VSEPR model.[85] Interestingly, the trend reverses for lead as the central atom, so the bond angles in PbX_2 are larger than in SnX_2. This can be interpreted in various ways. For example, the decreasing bond angle may reach a point at which the van der Waals and/or Coulomb nonbonded interactions will cause the ligands to get further away from each other and, hence, the bond angle will open somewhat. Another plausible explanation can be the

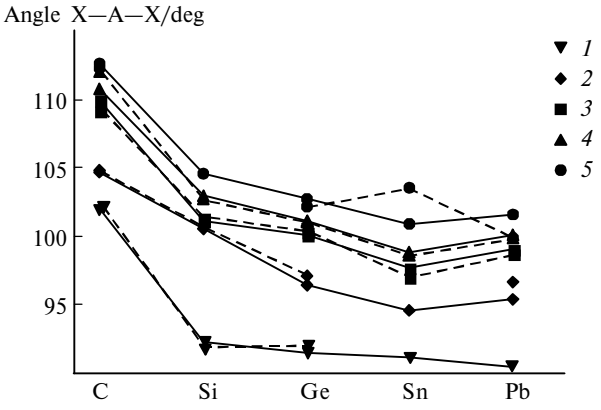

Fig. 3. Experimental (dashed lines) and computed (solid lines) bond angle variations in singlet ($^1A_1$) carbenes and carbene analogs AX_2 (A = C, Si, Ge, Sn, Pb): X = H (*1*), F (*2*), Cl (*3*), Br (*4*), and I (*5*).

Table 4. Calculated singlet—triplet energy gaps (ΔE_{S-T}) for carbene analogs AX_2 (A = Si, Ge, Sn, and Pb; X = H, F, Cl, Br, and I)

Species	ΔE_{S-T} /kJ mol^{-1}	Computational method	Reference
SiH_2	25.9	RHF	71
	87.8(42)	SOCI-f(D)	34
	89.3(4)	CCSD(T)	72
SiF_2	319.2	LDA/NL	28
	307.5	CISD	37
$SiCl_2$	160.9	HF	44
	230.9	DCCI	45
$SiBr_2$	139.7	HF	44
GeH_2	79.9	CI	73
	96.4	MCSCF/SOCI/RCI	49
GeF_2	346.4	CCSD(T)	53
	266.9	DFT	54
	310.0	CI	73
	336.7	MRSDCI(+Q)	52
$GeCl_2$	252.3	MRSDCI	57
	198.2	HF	44
	268.7	DFT	54
$GeBr_2$	232.2	MRSDCI	57
	174.2	HF	44
	242.1	DFT	54
GeI_2	177.4	MRSDCI	57
SnH_2	49.3	HF	71
	99.6	r_e, MCSCF/SOCI/RCI	49
SnF_2	312.07	MRSDCI+Q	52
$SnCl_2$	251.0	MRSDCI	63
$SnBr_2$	232.2	MRSDCI	63
SnI_2	197.1	MRSDCI	63
PbH_2	143.9	MCSCF/SOCI/RCI	49
PbF_2	400.4	MRSDCI+Q	52
$PbCl_2$	291.6	MRSDCI	63
$PbBr_2$	271.9	MRSDCI	63
PbI_2	225.0	MRSDCI	63

influence of relativistic effects on the large central lead atom. These effects cause the 6s-orbital to contract, leading to an increase in the electron density near the central atom, and this will cause the bond angle to open. This explanation is further supported by the fact that calculations performed without considering relativistic effects lead to a decrease in the bond angle, as should be expected. A similar phenomenon has been observed for the bond angle variation in the molecules of Group 15 element trihalides.[86] Of course, these alternative explanations do not exclude the presence of both effects; however, it is difficult to estimate their relative contributions at this point.

The bond angle variations for the triplet species AX_2 are presented in Fig. 4. The trend is similar to what has been observed for the singlet carbenes and their analogs, except for a considerable increase in the bond angle for the lead derivatives.

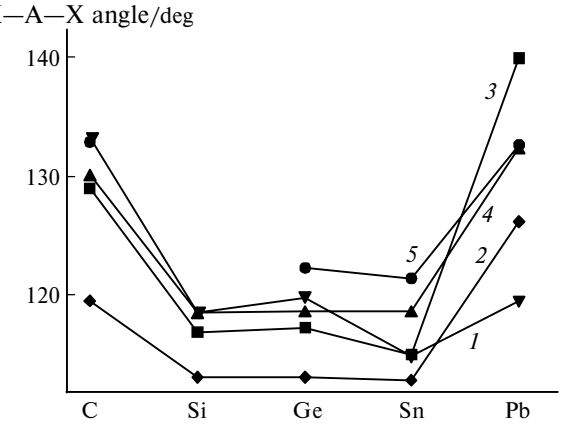

Fig. 4. Bond angle variations in triplet ($^3B_1$) carbenes and carbene analogs AX_2 (A = C, Si, Ge, Sn, Pb): X = H (*1*), F (*2*), Cl (*3*), Br (*4*), and I (*5*) from computation.

Comparison of the bond lengths, bond angles, and the relative energies of the corresponding singlet and triplet species with each other is also of interest. As mentioned above, methylene and all substituted carbenes have two relatively low-lying orbitals with a_1 and b_1 symmetry. Depending on how the electrons are arranged on them, we have either a singlet ($^1A_1$) or a triplet ($^3B_1$) state. The relative energies of these states depend on the substituents at the central atom and their electronic and steric interactions. For carbene and its derivatives, the a_1 orbital is an antibonding σ-orbital composed of the C s- and p-orbitals and X p-orbitals in opposite phase. In the case of highly electronegative ligands, the contribution of the carbon s-orbital to bonding increases. As a result, the energy of this orbital decreases, thus making electron pairing advantageous and leading to the singlet state. As to the geometry, the bond angles decrease due to electron withdrawal by the highly electronegative ligands, and this is what the VSEPR model[85] also anticipates.

Recently,[27] it has been discussed that CF_2 is characterized by the largest energy gap between the a_1 HOMO and b_1 LUMO in the series of CX_2 (X = F, Cl, Br, I, H) species and that the singlet state of difluorocarbene is much lower in energy than the triplet state. With decreasing ligand electronegativity, the contribution of the s-orbital to the a_1 orbital decreases and thus the energy of that orbital increases. As a consequence, the singlet—triplet energy gap decreases. This change in the orbital energies is accompanied by an opening of the bond angle on going from X = F to X = I, which is again in accordance with the VSEPR model.[85] Methylene, CH_2, for which the ground state is triplet, represents a special case.

The b_1 orbital is an antibonding orbital composed of both carbon and ligand p_π-orbitals. If the energies of these p_π-orbitals are comparable, they are strongly

Table 5. Experimental and calculated bond lengths (r) in the molecules of Group 14 element tetrahalides AX_4 (A = C, Si, Ge, Sn, and Pb; X = F, Cl, Br, and I)

Molecule	r(A—X)/Å	Physical meaning, method/level of theory, basis sets	Reference
CF_4		Experiment	
	1.3151(17)	r_e, IR + MW + Raman	74
		Calculations	
	1.3214	r_e, B3LYP/QR	19
	1.325	r_e, B3LYP/6-311+G(df)	21
CCl_4		Experiment	
	1.7667(30)	r_g, ED	75
		Calculations	
	1.7942	r_e, B3LYP/QR	19
CBr_4		Experiment	
	1.942(2)	r_g, ED	76
		Calculations	
	1.9616	r_e, B3LYP/QR	19
CI_4		Experiment	
	2.166(7)	r_g, ED	27
		Calculations	
	2.21	r_e, B3LYP/QR	19
SiF_4		Experiment	
	1.554(3)	r_a, ED	77
	1.5540423(17)	r_e, IR + MW	78
		Calculations	
	1.5699	r_e, B3LYP/QR	19
	1.562	r_e, CCSD(T)/aV5Z	33
$SiCl_4$		Experiment	
	2.0193(34)	r_g, ED	79
		Calculations	
	2.0466	r_e, B3LYP/QR	19
$SiBr_4$		Experiment	
	2.183(4)	r_g, ED	80
		Calculations	
	2.2204	r_e, B3LYP/QR	19
SiI_4		Calculations	
	2.4809	r_e, B3LYP/QR	19
GeF_4		Experiment	
	1.67(3)	r_a, ED	81
		Calculations	
	1.7183	r_e, B3LYP/QR	19
	1.685	r_e, BHLYP	51
	1.709	r_e, B3LYP	51
$GeCl_4$		Experiment	
	2.113(3)	r_g, ED	75
		Calculations	
	2.1623	r_e, B3LYP/QR	19
$GeBr_4$		Experiment	
	2.272(3)	r_g, ED	82
		Calculations	
	2.3269	r_e, B3LYP/QR	19
GeI_4		Calculations	
	2.5768	r_e, B3LYP/QR	19
SnF_4		Calculations	
	1.892	r_e, B3LYP/QR	19
$SnCl_4$		Experiment	
	2.2808(37)	r_g, ED	83
		Calculations	
	2.3358	r_e, B3LYP/QR	19
	2.291	r_e, MP2	64
	2.297	r_e, MP4	64
	2.301	r_e, QCISD	64
$SnBr_4$		Calculations	
	2.4898	r_e, B3LYP/QR	19
SnI_4		Calculations	
	2.7286	r_e, B3LYP/QR	19
PbF_4		Calculations	
	1.9624	r_e, B3LYP/QR	19
	1.924	r_e, HF/QRPP	66
$PbCl_4$		Experiment	
	2.369(2)	r_g, ED	84
		Calculations	
	2.381	r_e, HF/QRPP	66
	2.4342	r_e, B3LYP/QR	19
$PbBr_4$		Calculations	
	2.5868	r_e, B3LYP/QR	19
PbI_4		Calculations	
	2.8218	r_e, B3LYP/QR	19

Note. For abbreviations of experimental methods, see Note to Table 1.

antibonding and thus the energy of the b_1 orbital will increase. This is what happens in CF_2. On going toward the heavier halocarbenes the energy of the ligand p-orbitals increases, while the overlap with the carbon p-orbitals decreases, and this will decrease the energy of the b_1 orbital. Hence, the a_1 and b_1 orbitals gradually come closer together as we go from fluorine to hydrogen and the singlet—triplet energy gap decreases. It has been verified experimentally as well as computationally that for carbene, CH_2, the triplet state is the ground state.

There are a few intriguing controversies concerning the stabilities of singlet and triplet species. A photoelectron spectroscopic study[22] indicated a rather narrow singlet—triplet energy gap for CCl_2. Meanwhile, computations, even at very high levels of theory, could not reproduce the experimental value.[25] The same photoelectron spectroscopic study indicated that CI_2 also has a triplet ground state, although with a very small singlet—triplet energy gap, determined with a large uncertainty (-1 ± 3 kcal mol^{-1}).[22] On the other hand, according to an electron diffraction study,[27] the singlet was the ground state for CI_2. However, the energy difference between the singlet and triplet states could not be determined reliably. It can be either rather large (if only singlet species are present in the vapor) or very small, at most, about 1 kcal mol^{-1}, with a large uncertainty (if both singlet and triplet species are present in the vapor).

The singlet—triplet energy differences for the non-carbon AX_2 species follow the same trend in each AX_2 series, except that the non-carbon dihydrides have a

singlet ground state. In some cases, the energy gap values do not follow the general pattern, and this requires further study. However, this may also be merely a consequence of the different origins of the data.

Comparison of the geometries of singlet and triplet carbenes shows a rather large difference in the bond angles. The bond angle in all triplet AX_2 species is generally 10° to 30° larger than in the corresponding singlet species. This can, again, be rationalized by the VSEPR rules. In a singlet species, there is a nonbonding electron pair with large space requirement in the vicinity of the central atom as compared with the A—X bonding pairs. Therefore, the X—A—X angle will be smaller than 120°. On the other hand, a single electron on the central atom in the triplet species requires less space than the A—X bonding pair; hence, the bond angle should be larger than 120°. Comparing the bond angle differences between respective pairs, one can see that they are the smallest for fluorine-containing species and increase on going to heavier halides for each central atom, with the hydrides having the largest differences.

The dipole moments of the singlet species are always larger than those of the triplet species. This can be rationalized by their different geometries. Obviously, the larger bond angles in the triplet species imply smaller dipole moments.

The bond length variation in the molecules of the tetrahalides of Group 14 elements is, again, in accordance with expectations. Comparison of the bond lengths in the corresponding tetrahalides and dihalides shows that the carbon-containing molecules are different from the rest. For all carbon halides, the tetrahalides have longer bonds than the dihalides. Although this is contrary to expectation, it can be rationalized by the relatively small size of the central atom and thus by strong nonbonded interactions in the tetrahalides, which prevent a decrease in the bond lengths. For all the other AX_2—AX_4 pairs, the bonds in the tetrahalides are shorter than in the corresponding dihalides.

Although the general trends discussed here are expressed by the data listed in Tables 1—5, there are certain inconsistencies, possibly as a result of the different origins of the data compared. Therefore, it would be useful to have a more consistent set of molecular parameters in order to establish more reliable trends in the variations of different properties of this interesting class of substances.

We are grateful to the Hungarian Scientific Research Fund (Grant No. OTKA T025788) and to the Ministry of Education of Hungary (Grant No. FKEP 0364/1999) for financial support.

References

1. O. B. Ramsay, *Stereochemistry*, Heyden, London, 1981.
2. G. A. Olah, *A Life of Magic Chemistry: Autobiographical Reflections of a Nobel Prize Winner,* Wiley-Interscience, New York, 2001.
3. M. Hargittai and I. Hargittai, *Int. J. Quant. Chem.*, 1992, **44**, 1057.
4. H. Petek, D. J. Nesbitt, D. C. Darwin, P. R. Ogilby, C. B. Moore, and D. A. Ramsay, *J. Chem. Phys.*, 1989, **91**, 6566.
5. D. Das and S. L. Whittenburg, *J. Mol. Struct.* (*THEOCHEM*), 1999, **492**, 175.
6. C. D. Sherrill, T. J. Van Huis, Y. Yamaguchi, and H. F. Schaefer, III, *J. Mol. Struct.* (*THEOCHEM*), 1997, **400**, 139.
7. C. D. Sherrill, M. L. Leininger, T. J. Van Huis, and H. F. Schaefer, III, *J. Chem. Phys.*, 1998, **108**, 1040.
8. Y. Yamaguchi, C. D. Sherrill, and H. F. Schaefer, III, *J. Phys. Chem.,* 1996, **100**, 7911.
9. M. Schwartz and P. Marshall, *J. Phys. Chem., A*, 1999, **103**, 7900.
10. C.-H. Hu, *Chem. Phys. Lett.,* 1999, **309**, 81.
11. B. Hajgató, H. M. T. Nguyen, T. Veszprémi, and M. T. Nguyen, *Phys. Chem., Chem. Phys.,* 2000, **2**, 5041.
12. N. Russo, E. Sicilia, and M. Toscano, *J. Chem. Phys.*, 1992, **97**, 5031.
13. G. Herzberg and J. W. C. Johns, *J. Chem. Phys.*, 1971, **54**, 2276.
14. P. R. Bunker, P. Jensen, W. P. Kraemer, and R. Beardsworth, *J. Chem. Phys.,* 1986, **85**, 3724.
15. D. E. Woon and T. H. Dunning, *J. Chem. Phys.,* 1995, **103**, 4572.
16. W. H. Kirchhoff, D. R. Lide, Jr., and F. X. Powell, *J. Mol. Spectr.,* 1973, **47**, 491.
17. C. W. Mathews, *Can. J. Phys.*, 1967, **45**, 2355.
18. V. M. García, O. Castell, M. Reguero, and R. Caballol, *Mol. Phys.,* 1996, **87**, 1395.
19. S. Escalante, R. Vargas, and A. Vela, *J. Phys. Chem., A*, 1999, **103**, 5590.
20. K. Sendt and G. B. Bacskay, *J. Chem. Phys.,* 2000, **112**, 2227.
21. A. Ricca, *J. Phys. Chem., A*, 1999, **103**, 1876.
22. R. L. Schwartz, G. E. Davico, T. M. Ramond, and W. C. Lineberger, *J. Phys. Chem., A*, 1999, **103**, 8213.
23. M. Fujitake and E. Hirota, *J. Chem. Phys.,* 1989, **91**, 3426.
24. D. J. Clouthier and J. Karolczak, *Phys. Chem.,* 1989, **93**, 7542; D. J. Clouthier and J. Karolczak, *J. Chem. Phys.,* 1991, **94**, 1.
25. C. J. Barden and H. F. Schaefer, III, *J. Chem. Phys.*, 2000, **112**, 6515.
26. R. C. Ivey, P. D. Schulze, T. L. Leggett, and D. A. Kohl, *J. Chem. Phys.,* 1974, **60**, 3174.
27. M. Hargittai, G. Schultz, P. Schwerdtfeger, and M. Seth, *Struct. Chem.*, 2001, **12**, 377.
28. G. L. Gutsev and T. Zigler, *J. Chem. Phys.,* 1991, **95**, 7220.
29. A. Gobbi and G. Frenking, *J. Chem. Soc., Chem. Commun.,* 1993, 1162.
30. E. P. F. Lee, J. M. Dyke, and T. G. Wright, *Chem. Phys. Lett.,* 2000, **326**, 143.
31. C. Yamada, H. Kanamori, E. Hirota, N. Nishiwaki, N. Itabashi, K. Kato, and T. Goto, *J. Chem. Phys.,* 1989, **91**, 4582.
32. R. Escribano and A. Campargue, *J. Chem. Phys.,* 1998, **108**, 6249.
33. D. Feller and D. A. Dixon, *J. Phys. Chem., A*, 1999, **103**, 6413.
34. K. Balasubramanian and A. D. McLean, *J. Chem. Phys.,* 1985, **85**, 5117.
35. M. Spoliti, F. Ramondo, L. Bencivenni, P. Kolandaivel, and R. Kumaresan, *J. Mol. Struct.* (*THEOCHEM*), 1993, **283**, 73.

36. H. Shoji, T. Tanaka, and E. Hirota, *J. Mol. Spectr.,* 1973, **47**, 268; V. M. Rao, R. F. Curl, P. L. Timms, and J. L. Margrave, *J. Chem. Phys.,* 1965, **43**, 2557.
37. M. E. Colvin, R. S. Grev, H. F. Schaefer, III, and J. Bicerano, *Chem. Phys. Lett.,* 1983, **99**, 399.
38. R. D. Johnson, III, J. W. Hudgens, and M. N. R. Ashfold, *Chem. Phys. Lett.,* 1996, **261**, 474.
39. J. Karolczak, R. H. Judge, and D. J. Clouthier, *J. Am. Chem. Soc.*, 1995, **117**, 9523.
40. Z. L. Cai and J. L. Bai, *Chem. Phys.,* 1993, **178**, 215.
41. I. Hargittai, G. Schultz, J. Tremmel, N. D. Kagramanov, A. K. Maltsev, and O. M. Nefedov, *J. Am. Chem. Soc.,* 1983, **105**, 2895.
42. A. G. Gershikov, N. Yu. Subbotina, and M. Hargittai, *J. Mol. Spectr.,* 1990, **143**, 293.
43. M. Fujitake and E. Hirota, *Spectrochimica Acta*, 1994, **50A**, 1345.
44. J. M. Coffin, T. P. Hamilton, P. Pulay, and I. Hargittai, *Inorg. Chem.,* 1989, **28**, 4092.
45. S. K. Shin, W. A. Goddard, III, and J. L. Beauchamp, *J. Phys. Chem.*, 1990, **96**, 6963.
46. F.-T. Chau, D.-C. Wang, E. P. F. Lee, J. M. Dyke, and D. K. W. Mok, *J. Phys. Chem.*, *A*, 1999, **103**, 4925.
47. J. Karolczak, W. W. Harper, R. S. Grev, and D. J. Clouthier, *J. Chem. Phys.,* 1995, **103**, 2839.
48. M.-D. Su and S.-Y. Chu, *J. Am. Chem. Soc.,* 1999, **121**, 4229.
49. K. Balasubramanian, *J. Chem. Phys.*, 1988, **89**, 5731.
50. H. Takeo and R. F. Curl, Jr., *J. Mol. Spectr.*, 1972, **43**, 21.
51. Q. Li, G. Li, W. Xu, Y. Xie, and H. F. Schaefer, III, *J. Chem. Phys.*, 1999, **111**, 7945.
52. D. Dai, M. M. Al-Zahrani, and K. Balasubramanian, *J. Phys. Chem.*, 1994, **98**, 9233.
53. J. Karolczak, R. S. Grev, and D. J. Clouthier, *J. Chem. Phys.,* 1994, **101**, 891.
54. B. Delley and G. Solt, *J. Mol. Struct.* (*THEOCHEM*), 1986, **139**, 159.
55. G. Schultz, J. Tremmel, I. Hargittai, I. Berecz, S. Bohátka, N. D. Kagramanov, A. K. Maltsev, and O. M. Nefedov, *J. Mol. Struct.,* 1979, **55**, 207.
56. M. J. Tsuchiya, H. Honjou, K. Tanaka, and T. Tanaka, *J. Mol. Struct.*, 1995, **352/353**, 407.
57. M. Benavides-Garcìa and K. Balasubramanian, *J. Chem. Phys.*, 1992, **97**, 7537.
58. G. Schultz, J. Tremmel, I. Hargittai, N. D. Kagramanov, A. K. Maltsev, and O. M. Nefedov, *J. Mol. Struct.*, 1982, **82**, 107; G. Schultz, M. Kolonits, and M. Hargittai, *Struct. Chem.*, 2000, **11,** 161.
59. N. I. Giricheva, G. V. Girichev, S. A. Shlykov, V. A. Titov, and T. P. Chusova, *J. Mol. Struct.,* 1995, **344**, 127.
60. A. G. Gershikov, E. Z. Zasorin, A. V. Demidov, and V. P. Spiridonov, *Zh. Strukt. Khim.*, 1986, **27**, Iss. 3, 36 [*J. Struct. Chem.* (*USSR),* 1986, **27**, Iss. 3 (Engl. Transl.)].
61. A. Ya. Nasarenko, V. P. Spiridonov, B. S. Butayev, and E. Z. Zasorin, *J. Mol. Struct.* (*THEOCHEM*), 1985, **119**, 263.
62. K. V. Ermakov, B. S. Butayev, and V. P. Spiridonov, *J. Mol. Struct.,* 1991, **248**, 143.
63. M. Benavides-Garcia and K. Balasubramanian, *J. Chem. Phys.*, 1994, **100**, 2821.
64. T. S. Elicker, A. H. Edwards, A. Smith, and J.-M. Laurent, *J. Mol. Struct.*, 2000, **525**, 53.
65. A. V. Demidov, A. G. Gershikov, E. Z. Zasorin, V. P. Spiridonov, and A. A. Ivanov, *Zh. Strukt. Khim.*, 1983, **24**, Iss. 1, 9 [*J. Struct. Chem.* (*USSR),* 1983, **24**, Iss. 1 (Engl. Transl.)].
66. M. Knaupp and P. v. R. Schleyer, *J. Am. Chem. Soc.*, 1993, **115**, 1061.
67. V. I. Bazhanov, *Zh. Strukt. Khim.*, 1991, **32**,, Iss. 1, 54 [*J. Struct. Chem.* (*USSR),* 1991, **32**, Iss. 1 (Engl. Transl.)].
68. I. Hargittai, J. Tremmel, E. Vajda, A. A. Ishchenko, A. A. Ivanov, L. S. Ivashkevich, and V. P. Spiridonov, *J. Mol. Struct.*, 1977, **42**, 147.
69. A. A. Ishchenko, Yu. I. Tarasenko, and V. P. Spiridonov, *Struct. Chem.*, 1990, **1**, 217.
70. P. Jensen and P. R. Bunker, *J. Chem. Phys.*, 1988, **89**, 1327.
71. G. Olbrich, *Chem. Phys. Lett.*, 1980, **73**, 110.
72. J. M. L. Martin, *J. Phys. Chem.*, *A*, 1998, **102**, 1394.
73. J.-C. Barthelat, B. S. Roch, G. Trinquier, and I. Satge, *J. Am. Chem. Soc.*, 1980, **102**, 4080.
74. S. Brodersen, *J. Mol. Spectr.,* 1991, **145**, 331.
75. Y. Morino, Y. Nakamura, and T. Iijima, *J. Chem. Phys.*, 1960, **32**, 643.
76. H. Thomassen and K. Hedberg, *J. Mol. Struct.,* 1990, **240**, 151.
77. B. Beagley, D. P. Brown, and J. M. Freeman, *J. Mol. Struct.*, 1973, **18**, 337; K. Hagen and K. Hedberg, *J. Chem. Phys.*, 1973, **59**, 1549.
78. M. Takami and H. Kuze, *J. Chem. Phys.*, 1983, **78**, 2204.
79. R. R. Ryan and K. Hedberg, *J. Chem. Phys.*, 1969, **50**, 4986.
80. T. Iijima, H. Jimbo, and M. Taguchi, *J. Mol. Struct.*, 1986, **144**, 191.
81. A. D. Caunt, H. Mackle, and L. E. Sutton, *Trans. Faraday Soc.*, 1951, **47**, 943.
82. G. G. B. Souza and J. D. Wieser, *J. Mol. Struct.*, 1975, **25**, 442.
83. H. Fuji and M. Kimura, *Bull. Chem. Soc. Jpn.*, 1970, **43**, 1933.
84. A. Haaland, A. Hammel, K.-G. Martinsen, J. Tremmel, and H. V. Volden, *J. Chem. Soc.*, *Dalton Trans.*, 1992, 2209; T. Strand, *Acta Chem. Scand.*, 1994, **48**, 960.
85. R. Gillespie and I. Hargittai, *The VSEPR Model of Molecular Geometry*, Allyn and Bacon, Boston, 1991.
86. M. Hargittai, *Chem. Rev.*, 2000, **100**, 2233.

Received June 13, 2001